PCCP

Accepted Manuscript

ROYAL SOCIETY OF CHEMISTRY

www.rsc.org/pccp

Modification of the surface chemistry of single- and multi-walled carbon nanotubes by HNO_3 and H_2SO_4 hydrothermal oxidation for application on direct contact membrane distillation

Sergio Morales-Torres, Tânia L.S. Silva, Luisa M. Pastrana-Martínez, Ana T.S.C. Brandão, José L. Figueiredo, Adrián M.T. Silva*

LCM - Laboratory of Catalysis and Materials - Associate Laboratory LSRE/LCM, Faculdade de Engenharia, Universidade do Porto, Rua Dr. Roberto Frias, 4200-465 Porto, Portugal.

*Corresponding author e-mail address: adrian@fe.up.pt (A.M.T. Silva)

Broader context

Fresh water supplies have always been scarce and a huge increase (ca. 20%) in the number of people facing water scarcity around the world has been estimated. Desalination is an excellent solution. We recently developed a novel HNO_3 hydrothermal oxidation methodology for functionalization of carbon materials, which allows fine control of the amount of oxygenated surface groups. However, this methodology was never used to prepare materials for real applications. In the present work, for the first time, we have: (i) compared single-walled CNTs with different lengths, and multi-walled CNTs, functionalized by this methodology; (ii) adapted the methodology to the use of H_2SO_4 (instead of only HNO_3), controlling the sulphur containing surface groups; and (iii) demonstrated the effect of the controlled surface chemistry of CNTs in a real application (desalination). It was found that the permeate flux correlated precisely with the amount of surface groups (as well as with the pH of point of zero charge) of the CNTs. The developed methodologies are of interest for many other applications, since it is well known that the surface properties of CNTs play a crucial role into a broader context, such as catalysis for water and air treatment, energy storage, sensors, fuel cells, photovoltaics, among others.

Abstract

A specific methodology based on nitric acid hydrothermal oxidation was used to control the surface chemistry of multi-walled (MWCNTs) and single-walled (SWCNTs) carbon nanotubes (CNTs) with different lengths, and this methodology was adapted to the use of sulphuric acid containing ammonium persulfate as oxidizing agent.

The amount of oxygen-containing surface groups depends on the number and length of the graphene layers of the CNTs, thicker and shorter CNTs having more reactive sites for surface functionalization. In particular, the oxidation of MWCNTs was more pronounced than that obtained for short SWCNTs and less surface groups were introduced in long SWCNTs, regardless of the acid used at any fixed concentration. It was also possible to tailor the surface chemistry of both SWCNTs and MWCNTs by using the adopted methodologies, and the amount of both oxygen- and sulphur-containing functional groups was correlated with the concentration of each oxidizing agent used. Mathematical functions that allow precise control of the amount and type of the surface groups introduced into carbon nanotubes were obtained.

Buckypapers were also prepared over a polytetrafluoroethylene commercial membrane. These membranes were tested in direct contact membrane distillation and, under salinity conditions, the membrane prepared with oxidized MWCNTs (instead of SWCNTs) was the most efficient, the permeate flux of the commercial membrane significantly increasing by the presence of these CNTs, while completely rejecting chloride ions. In addition, the permeate flux was precisely correlated with the amount of oxygenated functional surface groups (as well as with the pH of point of zero charge) of the oxidized MWCNTs.

Keywords: *carbon nanotubes, hydrothermal oxidation, surface chemistry, buckypapers, membrane distillation.*

1. Introduction

The attention on nanostructured carbon materials, such as fullerenes (C_{60}), carbon nanotubes (CNTs) and more recently, graphene, has increased over the years. In particular, since the work published by Iijima in 1991,[1] CNTs have attracted a large interest in nanoscience and nanotechnology. The electrical properties, mechanical resistance and thermal conductivity of CNTs are responsible by their use in several applications, such as energy storage, electronics, sensors, catalysis and separation processes, including desalination.[2-4]

The preparation of structured materials based on CNTs requires an adequate dispersion of CNTs in a solvent and, when this solvent is water, the predominantly hydrophobic nature of the carbon material might be a drawback. Chemical functionalization is an efficient method to turn CNTs more hydrophilic and soluble, as well as to control the acidic and basic character of CNTs, and can be performed either in the gas or liquid phase. Typical gas phase oxidants are oxygen, steam, ozone or carbon dioxide,[5, 6] while most of the liquid phase methods are based on nitric acid (HNO_3),[7-9] sulphuric acid (H_2SO_4),[10] mixtures of both (HNO_3/H_2SO_4),[11] "piranha" solution (H_2O_2/H_2SO_4)[12, 13] or potassium permanganate ($KMnO_4$).[14]

In the particular case of liquid phase treatments, refluxing/boiling the oxidizing agent (high concentration) over long periods of time is the conventional approach to functionalize CNTs. Besides the creation of oxygenated functional groups on the tube edges and sidewall defects of the CNTs, other structural effects or changes can take place, such as: oxidation of amorphous carbon; removal of the particles of catalyst used to grow CNTs by chemical vapor deposition (CVD); expansion of the CNTs bundles and formation of new bundles by isolated CNTs; opening of the tube tips and shortening of the tubes as well as fragmentation of side walls to yield acidic carboxylated carbon fragments (CCFs).[8, 15]

Therefore, the modification of the surface chemistry of CNTs by using liquid-phase oxidizing agents is not a recent issue. However, methodologies and protocols for tailoring the surface chemistry of CNTs which employ low concentrations of oxidizing agents, thus avoiding significant structural changes of CNTs and minimizing the costs and environmental

concerns associated to these methodologies, are still needed.[16] It has been shown that precise amounts of oxygenated functional groups (−OH, −C=O and −COOH) can be introduced on the surface of SWCNTs and MWCNTs by the HNO_3 hydrothermal oxidation methodology,[17-19] employing significantly lower concentrations of HNO_3 than conventional boiling methods, and achieving comparable or even higher efficiency in the amount of oxygenated surface groups that are introduced. This was proved by combining several powerful and complementary techniques for the characterization of the surface groups after hydrothermal oxidation, such as temperature programmed desorption (TPD), Raman spectroscopy, thermogravimetric analysis and water adsorption/desorption.[18]

The chemical oxidation of CNTs is of particular relevance when these carbon materials are used to prepare membranes for desalination. As an example, MWCNTs treated with nitric/sulphuric acid were found to perform better in direct contact membrane distillation (DCMD) than with the non-functionalized analogues.[20] In the DCMD process, a hydrophobic membrane acts as a barrier between seawater (hot - feed) and fresh water (cold - permeate), and the vapour pressure difference generated between both sides of the membrane drives water vapour from the hot side to the cold side, where it condenses. The improvement on the performance of the process was attributed to the polar surface groups which provided higher sorption of the water vapour molecules, resulting in an increase of the permeate flux.[20] However, most of the works reported in literature have not considered the effect of CNTs functionalization on the desalination performance with DCMD. For instance, buckypapers (BPs), thin sheets consisting of randomly oriented CNTs, were prepared with pristine MWCNTs (assembled by van der Waals forces only) and tested as self-supporting membranes in DCMD, reaching high permeability and salt rejection but also presenting short lifespan.[21] Pristine MWCNTs have been also used to prepare BPs that were then hot-pressed with polymeric membranes, such as polypropylene and polytetrafluoroethylene (PTFE), or infiltrated with polymers, e.g. polyvinyldifluoride and polystyrene, the respective lifespan and salt rejection often increasing but the permeate flux being maintained.[22, 23] The limited

performance of BP membranes prepared with CNTs in comparison with commercial PTFE membranes (used as reference in DCMD) has been justified by the small pore size distribution found in BPs and by the high thermal conductivity of CNTs.[24]

Overall, to the best of our knowledge, the performance of the DCMD process when using BPs prepared with CNTs with different amounts of oxygenated surface groups was not investigated so far. Therefore, in the present work, HNO_3 hydrothermal oxidation of MWCNTs and SWCNTs with different lengths is compared for the first time, and this methodology was adapted to the use of H_2SO_4 (containing ammonium persulfate - $(NH_4)_2S_2O_8$) as oxidizing agent. The surface chemistry of these CNTs is characterized in detail, and the different functional groups created on their surface are identified and quantified in order to develop methodologies for precise control of the surface chemistry of these carbon materials. BPs were then prepared over a commercial PTFE membrane, using both MWCNTs and SWCNTs (either pristine or oxidized), and tested in DCMD of salty and distilled water. The influence of the CNTs surface chemistry on the permeate flux and salt rejection of these BP membranes was assessed, and their performances compared with a commercial PTFE membrane.

2. Experimental section

2.1. Carbon nanotubes

Pristine CNTs prepared by CVD were purchased from Nanocyl™ (MWCNTs, NC3100 series with carbon purity > 95 wt.%) and Cheaptubes Inc. (SWCNTs, long and short with references Sku-0101 and Sku-0104, respectively, and purity higher than 90 wt.%). Table 1 shows some properties of these materials that were provided by the manufacturers. In the particular case of the SWCNTs samples, the content of MWCNTs is around 5 wt.% and the amorphous carbon content lower than 3 wt.%. The pristine MWCNTs, short SWCNTs and long SWCNTs will be referred hereafter as pristine MW, SW/S and SW/L, respectively.

Table 1. Properties of CNTs used in this work.

Label	Type of CNTs	Outer diameter (nm)	Inner diameter (nm)	Average length (μm)	Ash content (wt.%)
MW	MWCNTs	9.5*	n.p.	1.5	3.9
SW/L	Long SWCNTs	1 – 2	0.8 - 1.6	5 – 30	3.8
SW/S	Short SWCNTs	1 – 2	0.8 - 1.6	0.5 – 2	4.0

*average diameter; n.p.: not provided

2.2. Functionalization of carbon nanotubes

The experimental procedure for the chemical functionalization of CNTs was adapted from that described in our previous publications,[16-18] but in the present work a stainless-steel autoclave (Parr Instruments, USA Mod. 4748) with 125 mL of total volume was used. In a typical oxidation experiment, 75 mL of acid solutions with concentrations ranging from 0.05 to 0.30 mol L^{-1} (in the case of SW/L, a single concentration of 0.30 mol L^{-1} was used) were transferred to a PTFE vessel and 0.2 g of the corresponding CNTs were added. Two types of acid solutions were used to perform the chemical functionalization: (i) a HNO_3 solution (prepared from 65 wt.% HNO_3, Fluka) and (ii) a H_2SO_4 solution with $(NH_4)_2S_2O_8$ (prepared from 95 wt.% H_2SO_4 and > 98 wt.% $(NH_4)_2S_2O_8$, Sigma-Aldrich) in a ratio of 7:3. The PTFE vessel was placed into the stainless-steel autoclave, which was sealed and placed in an oven at 473 K for 2 h. This temperature was selected in our previous study with other SWCNTs (length of 5 - 15 μm).[17] After heat treatment, the autoclave was allowed to cool until room temperature. The recovered CNTs were washed several times with distilled water to remove the excess of acid until a neutral pH was achieved in the rinsing water and then dried overnight at 393 K. Additionally, a blank test was performed with distilled water, instead of the acid solutions, maintaining the other experimental parameters. The oxidized samples are labelled as X-Y-Z, where X is the type of CNTs used, namely MW (MWCNTs), SW/S (short SWCNTs) or SW/L (long SWCNTs); Y is the type of oxidizing agent, HN (for HNO_3) or HS (for H_2SO_4 containing $(NH_4)_2S_2O_8$); and Z is the acid solution concentration in mol L^{-1} (i.e. 0.05, 0.10,

0.20 or 0.30). CNTs treated with deionized water only, i.e. blank experiments, are labelled as blank-X, where X refers to the type of CNTs used (MW, SW/S or SW/L).

2.3. Characterization of carbon nanotubes

Thermogravimetric (TG) and differential thermogravimetric (DTG) analyses of the materials were performed by heating the sample in nitrogen flow from 323 to 1173 K at 20 K min^{-1} using a STA 490 PC/4/H Luxx Netzsch thermal analyser. The weight loss obtained under these experimental conditions was considered as the amount of volatiles.

Textural characterization of CNTs was obtained from the nitrogen adsorption-desorption isotherms determined at 77 K in Quantachrome NOVA 4200e and Quantachrome autosorb-iQ2 instruments. Before the analysis, all samples were outgassed for 8 h at 393 K. The apparent surface area (S_{BET}) was determined by applying the Brunauer-Emmett-Teller (BET) equation.[25] The BJH method[26] was applied to the desorption branch of the nitrogen isotherms in order to obtain the average pore diameter (d_{Pore}), mesopore volume (V_{Meso}) and the total pore volume (V_{Pore}). Pore size distributions (PSD) and micropore volume (V_{Micro}) of some selected samples were determined by using the quenched solid density functional theory (QSDFT), nitrogen - carbon equilibrium transition kernel at 77 K of Quantachrome's Library.[27] In contrast to other models based on non-local density functional theory (NLDFT), the QSDFT model takes into account the surface geometrical heterogeneity (i.e. roughness), which is influenced by the oxidation treatments performed on the materials, and eliminates gaps (namely in the regions of ~1 and ~2 nm) that are typical artifacts of the NLDFT theory, because this model deals with the pore walls as homogeneous graphite-like plane surfaces.

The surface chemistry was determined by the point of zero charge (pH_{PZC}) and by temperature programmed desorption (TPD). The measurements of pH_{PZC} of the materials were determined following a pH drift method described elsewhere.[28, 29] Firstly, nitrogen was bubbled in distilled water to prevent carbon dioxide dissolution and respective water acidification. Then, solutions with varying initial pH (2–9) were prepared using HCl (0.1 mol L^{-1}) or NaOH

(0.1 mol L^{-1}) and 20 mL of NaCl (0.01 mol L^{-1}) as electrolyte. After that, CNTs (0.05 g) were added to these solutions and left under stirring for 48 h at 298 K. The final pH was measured and plotted against the initial pH, determining by this way the pH_{PZC}, i.e. the pH value where initial pH = final pH.

TPD spectra were recorded with an automated AMI-300 apparatus for catalyst characterization (Altamira Instruments) equipped with a quadrupole mass spectrometer (Ametek, Mod. Dymaxion) and following the experimental procedure described elsewhere.[30, 31] In a typical experiment, CNTs (0.10 g) were placed in a U-shaped quartz tube inside an electrical furnace and heated under a constant helium flow of 25 cm^3 min^{-1} (STP), at 5 K min^{-1} up to 1373 K. Selected mass signals, m/z = 18, 28, 44, 48 and 64 were monitored during the thermal analysis. The amounts of CO and CO_2 were calibrated at the end of each analysis with CO and CO_2 gases, while SO_2 was calibrated with a sulphanilamide standard (which releases SO_2 upon thermal degradation), as referred elsewhere.[32] Since one of the fragments in the mass spectrum of CO_2 occurs at m/z = 28, the mass signal monitored for quantification of CO (m/z = 28) was corrected in order to eliminate the influence of CO_2 on CO evolution.[30, 31] The mass signal corresponding to the release of SO (m/z = 48) was also monitored, since it contributes to the mass spectrum of SO_2 with a peak intensity of 49% to that of SO_2.[33]

2.4. Preparation of the buckypapers

PTFE membranes (Fluopore™) with 0.22 μm pore size and diameter of 25 mm were purchased from Millipore, consisting of a thin (~30 μm) layer of PTFE bonded to a high-density polyethylene support. Pristine and oxidized CNTs were selected to prepare the corresponding BPs following a methodology adapted from elsewhere.[21] In a typical procedure, CNTs were dispersed in a 1g L^{-1} propan-2-ol solution during 20 min by using an ultrasonic processor (UP400S, 24 kHz). Then, the PTFE membrane was placed into a filtration device under vacuum and 5 mL of the dispersion was added four times in intervals of 5 min (a total of 20 mL) to favour the homogeneous deposition of CNTs (ca. 200 mg) and the stable formation

of a buckypaper. The BP membranes were placed between two cellulose papers and dried by controlled heating until 373 K in an oven.

2.5. Direct contact membrane distillation

The prepared BPs and the reference PTFE membrane were tested in a home-made built unit of DCMD (Scheme 1). In a typical run, with salty water, the membrane was placed into a "H-shape" glass DCMD module operating in cross-flow (effective membrane area of 2 cm^2). Then, salty (35 g L^{-1} of NaCl - feed) and distilled (DI - permeate) waters were pumped in recirculation mode through heat and cool exchangers, respectively, at similar flow rates (ca. 50 mL min^{-1}). The temperature at both sides of the DCMD module was continuously monitored by two thermocouples and maintained at 355 K (feed) and 293 K (permeate), resulting in a pressure difference of 54 kPa between both sides of the membrane. Ionic conductivity was measured in both feed and permeate streams by using online conductivity meters (VWR mod.310) and ion chromatography (Metrohm, mod. 881 Compact IC pro) to determine the percentage of salt rejection. The permeate flux (J) of the membranes was calculated by Eq. (1):

$$J = \Delta W/(S \times \Delta t) \quad (1)$$

where J is the permeate flux (kg s^{-1} m^{-2}), ΔW is the mass of distillate (kg), S is the effective area of the membrane (m^2), and Δt is the sampling time (seconds). Experiments were also performed using DI water at both sides of the membrane.

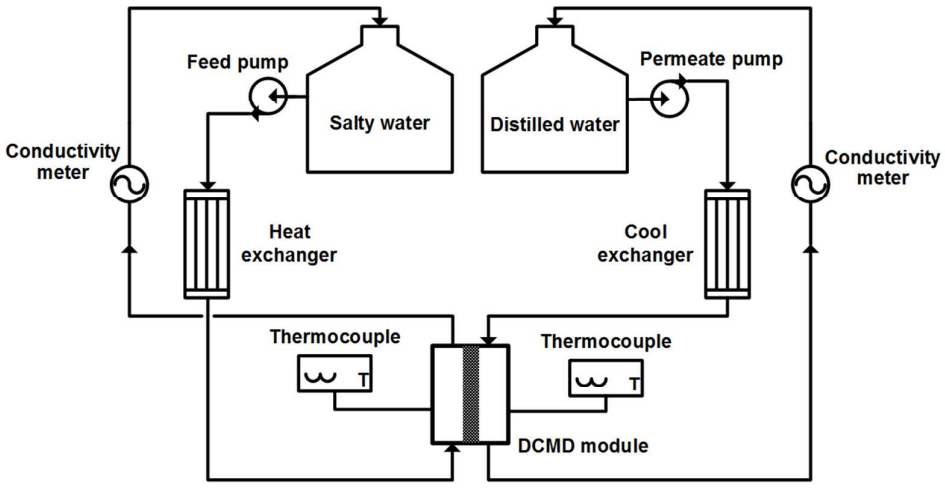

Scheme 1. Schematic representation of the DCMD unit.

3. Results and discussion

3.1. Volatile content and weight loss of the materials

The amount of volatiles present in the CNTs surface was determined by TG analysis and the results are shown in Figures 1a and 1b for the treatments with H_2SO_4 and HNO_3, respectively. The volatile content can be attributed to the amount of groups created on the CNT surface and evolved upon heating the sample under inert gas flow. This value gives qualitative information about the impact of the oxidation treatments on the chemical properties of CNTs. Thus, different results are obtained depending on the kind of CNTs and oxidizing agent used, but an increase of the amount of volatiles with the acid concentration is always observed. In fact, the volatile content can be correlated by a mathematical function with the acid concentration, a dependency of the oxidation process being found with the acid concentration and in agreement with our previous works.[16, 17]

The amount of volatiles determined by TG for SW/L treated with HNO_3 (8.5 wt.% for SW/L-HN-0.30 in Figure 1a) and H_2SO_4 (4.6 wt.% for SW/L-HS-0.30 in Figure 1b) was larger than that determined in the blank experiment using water only (3.4 wt.%), indicating that functional surface groups were created with the acid treatments. In addition, the volatile contents of all samples were more significant when HNO_3 (Figure 1b) was used instead of H_2SO_4 (Figure 1a) and, consequently, a larger amount of functional groups was introduced by HNO_3. For instance, the amounts of volatiles (wt.%) for MW-HN-0.30, SW/S-HN-0.30 and SW/L-HN-0.30 were 11.5%, 11.0% and 8.5%, respectively, while 6.1%, 5.0% and 4.6% were obtained for the corresponding CNTs treated with 0.30 mol L^{-1} of H_2SO_4. The amount of volatiles seems to be also dependent on the kind of CNTs used, i.e. the length (SW/S *vs.* SW/L) or the number of the graphene layers (SW/S *vs.* MW), as follows: MW > SW/S > SW/L for each acid (regardless of the concentration used in the oxidation treatments of MW and SW/S). Yu et al.[34] also reported that the degree of oxidation obtained, in this case by refluxing with 9 M HNO_3, depends on the kind of CNTs used, higher amounts of volatiles being obtained for MWCNTs in comparison to SWCNTs.

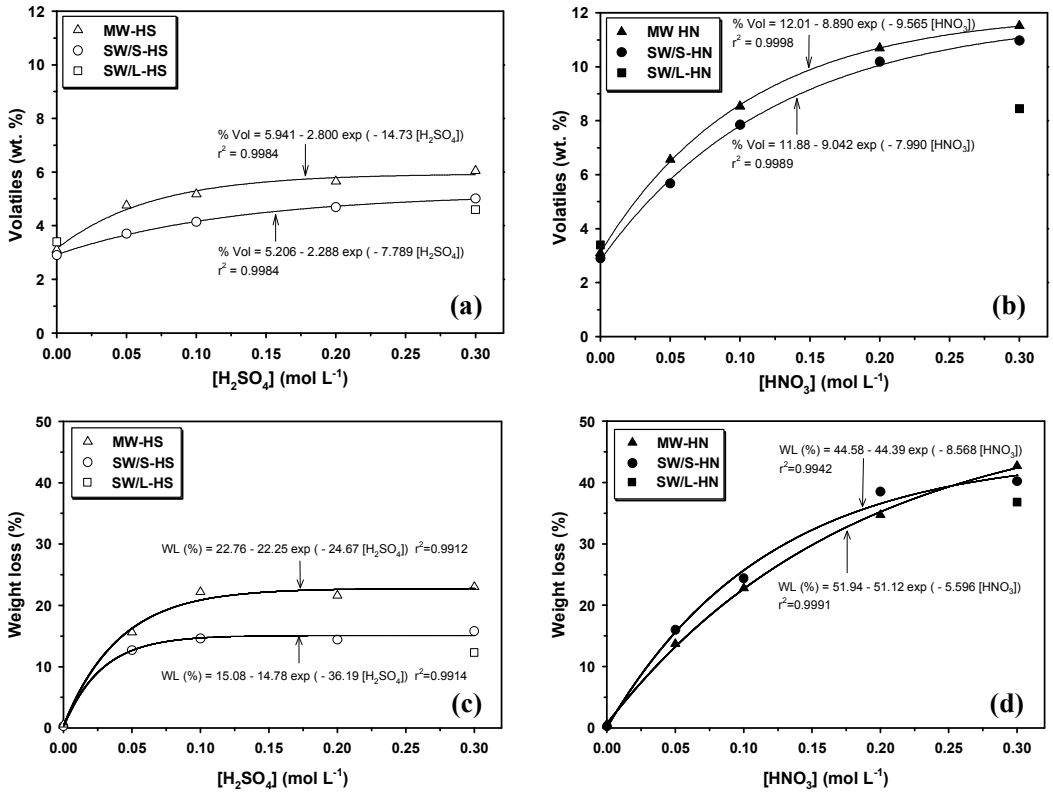

Figure 1. Volatile content (wt.%) of MW and SW/S treated with different (a) H_2SO_4 or (b) HNO_3 concentrations (the corresponding data for blank SW/L (using water only) and SW/L treated at 0.30 mol L^{-1} concentration are also included for comparison), and weight loss (WL) obtained after oxidation treatments with different (c) H_2SO_4 or (d) HNO_3 concentrations for all CNTs studied.

The weight loss (WL) for all CNTs after the oxidation treatments with different oxidizing agents and at different acid concentrations is shown in Figures 1c and 1d. The WL for blank experiments (i.e. CNTs only treated with deionised water instead of acid solution) was negligible, independently of the CNTs studied. This means that CNTs are not affected by the thermal treatment when an oxidizing agent is not used.

In the same way observed for the amount of volatiles, the WL increases with the acid concentration, both for MW and SW/S, a mathematical function fitting each set of experimental data. Therefore, the oxidation process seems to be directly related with the acid concentration. Different trends of the WL are observed depending on the kind of oxidizing agent used; in general, a clear increase is observed when HNO_3 is used (Figure 1d) to functionalize both MW and SW/S materials, while a plateau appears when H_2SO_4 is used at

concentrations higher than 0.10 mol L^{-1} (Figure 1c). In addition, the WL obtained for all the CNTs treated with HNO_3 was always higher than that determined for the CNTs treated with H_2SO_4, which can be indicative of a stronger oxidation by HNO_3. For instance, for an acid concentration of 0.30 mol L^{-1}, the WL (wt.%) decreased in the order: MW-HN (43%) ≈ SW/S-HN (40%) > SW/L-HN (37%) > MW-HS (23%) > SW/S-HS (16%) > SW/L-HS (12%), following a similar trend to that described for the amount of volatiles. The high WL values obtained for the CNTs oxidized with HNO_3 could be explained by the initial formation of carbon fragments[9] that are fully gasified by the action of this strong oxidant.[34]

Differences in the WL are also observed depending on the kind of CNTs used. In general, for a given concentration of oxidizing agent, the WL for MW was higher than for SW/S, and the lowest WL was obtained for SW/L. Thus, the number of graphene layers (MW *vs.* SW/S) and the length of CNTs (SW/S *vs.* SW/L) affect the amount of groups introduced in CNTs by the hydrothermal process.

3.2. Influence of the oxidation treatments on the textural properties of CNTs

Controlled oxidation leads to the incorporation of different oxygenated functionalities which are expected to influence the textural properties of CNTs. The textural properties of all CNTs are shown in Figures S1 and S2, as well as in Table 2.

The nitrogen isotherms for MW treated at different H_2SO_4 concentrations (Figure S1a) can be classified as type II according to the IUPAC classification,[35] which are typical of non-porous materials. The S_{BET} for MW treated with H_2SO_4 are higher than for pristine MW (Table 2) and, in general, seem to increase with the H_2SO_4 concentration used (e.g., S_{BET} = 315 and 437 m^2 g^{-1} for pristine MW and MW-HS-0.30, respectively). This increase of S_{BET} could be due to the oxidation of amorphous carbon present on the bundles.[15, 36] The materials treated with HNO_3 presented also a higher S_{BET} (> 400 m^2 g^{-1}) than the pristine MW, but a different behaviour is observed for their nitrogen isotherms (Figure S1b), mainly at the high relative pressures, where a decrease of nitrogen uptake (i.e., total pore volume) is recorded with the

increase of the HNO_3 concentration, besides the formation and shift of the hysteresis loop towards lower relative pressures (typical of materials with type IV isotherms). In this case, S_{BET}, V_{Meso} and V_{Pore} in general decreased with the increase of HNO_3 concentration. In addition, d_{Pore} decreased (Table 2, Figure S3a) for all oxidized MW materials, in comparison with pristine MW (e.g., 46, 18 and 13 nm for pristine MW, MW-HN-0.10 and MW-HN-0.30, respectively). This could be explained on the basis of more efficient packing of the CNTs due to excess hydrogen bonding between functional groups, leading to thicker bundles.[8, 18] These effects are more notorious when HNO_3 is used as oxidizing agent (Figure S3a).

Table 2. Textural properties of pristine and treated CNTs.

Sample	S_{BET} (± 5 m^2 g^{-1})	V_{Meso} (± 0.01 cm^3 g^{-1})	V_{Pore} (± 0.01 cm^3 g^{-1})	d_{Pore} (± 1 nm)
Pristine MW	315	1.89	2.31	46
MW-HS-0.05	364	2.29	2.37	32
MW-HS-0.10	354	2.15	2.24	32
MW-HS-0.20	382	2.10	2.20	32
MW-HS-0.30	437	2.21	2.32	32
MW-HN-0.05	449	1.39	1.41	25
MW-HN-0.10	465	1.06	1.07	18
MW-HN-0.20	436	0.70	0.70	13
MW-HN-0.30	400	0.64	0.65	13
Pristine SW/S	437	0.60	0.63	6.2
SW/S-HS-0.05	378	0.61	0.74	6.2
SW/S-HS-0.10	361	0.62	0.76	6.2
SW/S-HS-0.20	410	0.51	0.55	6.2
SW/S-HS-0.30	387	0.49	0.54	6.2
SW/S-HN-0.05	390	0.44	0.47	< 2.0
SW/S-HN-0.10	403	0.42	0.43	< 2.0
SW/S-HN-0.20	353	0.34	0.35	< 2.0
SW/S-HN-0.30	306	0.30	0.31	< 2.0
Pristine SW/L	450	1.02	1.28	46
SW/L-HS-0.30	409	0.94	1.00	32
SW/L-HN-0.30	330	0.75	0.83	32

In the case of the nitrogen adsorption isotherms for pristine SW/S and for SW/S treated with H_2SO_4, the main differences between them are also related with the volume of nitrogen

adsorbed at high relative pressures and S_{BET} which decreased with the increase of acid concentration (Figure S1c and Table 2). The textural changes of these CNTs were more evident when HNO_3 was used as oxidizing agent, both for nitrogen uptake (Figure S1d) and S_{BET} (437, 387 and 306 $m^2\ g^{-1}$, for pristine SW/S, SW/S-HS-0.30 and SW/S-HN-0.30, respectively). The results for SW/L oxidized with 0.30 mol L^{-1} of H_2SO_4 or HNO_3 lead to similar conclusions; i.e. the nitrogen uptake in the adsorption isotherms at high relative pressures (Figure S2) as well as S_{BET} (450, 409 and 330 $m^2\ g^{-1}$, for pristine SW/L, SW/L-HS-0.30 and SW/L-HN-0.30, respectively) are lower for SW/L treated with HNO_3 in comparison with H_2SO_4, as also V_{Meso} and V_{Pore}. In addition, oxidized SW/L presented always higher S_{BET} than the corresponding SW/S treated with the same concentration of acid, regardless of the acid used (i.e., S_{BET} = 409 and 387 $m^2\ g^{-1}$ for SW/L-HS-0.30 and SW/S-HS-0.30, and 330 and 306 $m^2\ g^{-1}$ for SW/L-HN-0.30 and SW/S-HN-0.30, respectively).

The pore size distribution (PSD) was calculated by applying QSDFT to the isotherm data. The QSDFT PSDs for pristine SWCNTs and treated with the highest acid concentration (0.30 mol L^{-1}) are shown in Figure S3. The QSDFT PSDs for pristine SW/S (Figure S3b) and SW/L (Figure S3c) were quite different, since SW/S presented two peaks centered at 0.93 and 1.54 nm, while SW/L showed a broad micropore distribution. However, the micropore volume calculated from QSDFT PSDs was comparable for both materials (V_{Micro} = 0.097 and 0.109 $cm^3\ g^{-1}$ for pristine SW/S and SW/L respectively). The micropore sizes determined could be due to the adsorption of nitrogen inside the tubes and/or into the interstitial channels of several tubes.[37, 38]

Concerning the mesopores (groove and external surface) resulting from the packing of the pristine SWCNTs bundles, both samples presented mesopores centred at 3.1 nm, pores with a larger size (10 nm) being only detected for SW/L, suggesting a different packing of SWCNTs with different lengths. In general, and in accordance with the previous discussion, the oxidation treatments produced a decrease of the microporosity (e.g., V_{Micro} = 0.097, 0.075 and 0.066 $cm^3\ g^{-1}$, for pristine SW/S, SW/S-HS-0.30 and SW/S-HN-0.30, respectively). In addition, the

impact of HNO_3 on the microporosity was higher than that observed with H_2SO_4, a lower micropore volume being determined for the SWCNTs treated with HNO_3 (e.g., V_{Micro} = 0.098 and 0.087 cm^3 g^{-1}, for SW/L-HS-0.30 and SW/L-HN-0.30, respectively). Changes in the mesopore range were also observed, a smaller mesopore volume being generally obtained for oxidized SW materials and mainly for those treated with HNO_3.

3.3. Analysis of the oxygenated functional groups created on the surface of CNTs

The surface chemistry of the different CNTs was analysed by TPD, significant information being obtained about the kind of functional groups incorporated on the treated CNTs. The TPD spectra, the total amounts of CO and CO_2, as well as the O_2 content, are summarized in Figure 2 (at different y-scales) and Table 3, while deconvolution of the TPD spectra for identification and quantification of the different oxygenated functional groups is shown and discussed in Section 3.5.

Figures 2a and 2b show the TPD spectra corresponding to the groups evolved as CO and CO_2, respectively, for pristine MW, for the blank experiment with deionized water and for MW treated under different H_2SO_4 concentrations. Comparing the desorption profiles it is evident that the incorporation of oxygenated groups is due to the presence of the acid, and that larger amounts of CO and CO_2 are released for higher H_2SO_4 concentrations (1312 and 471 μmol g^{-1}, respectively, for MW-HS-0.30). A similar effect was observed for MW treated with HNO_3 (Figures 2c and 2d, for CO and CO_2, respectively), i.e., larger amounts of CO and CO_2 were released when the HNO_3 concentration was increased (respectively up to 3535 and 1216 μmol g^{-1} for MW-HN-0.30). Comparing MW treated with H_2SO_4 (Figures 2a and 2b) and HNO_3 (Figures 2c and 2d), significantly larger amounts of oxygenated surface groups were produced with HNO_3. Therefore, under the employed experimental conditions, HNO_3 is a stronger oxidizing agent.

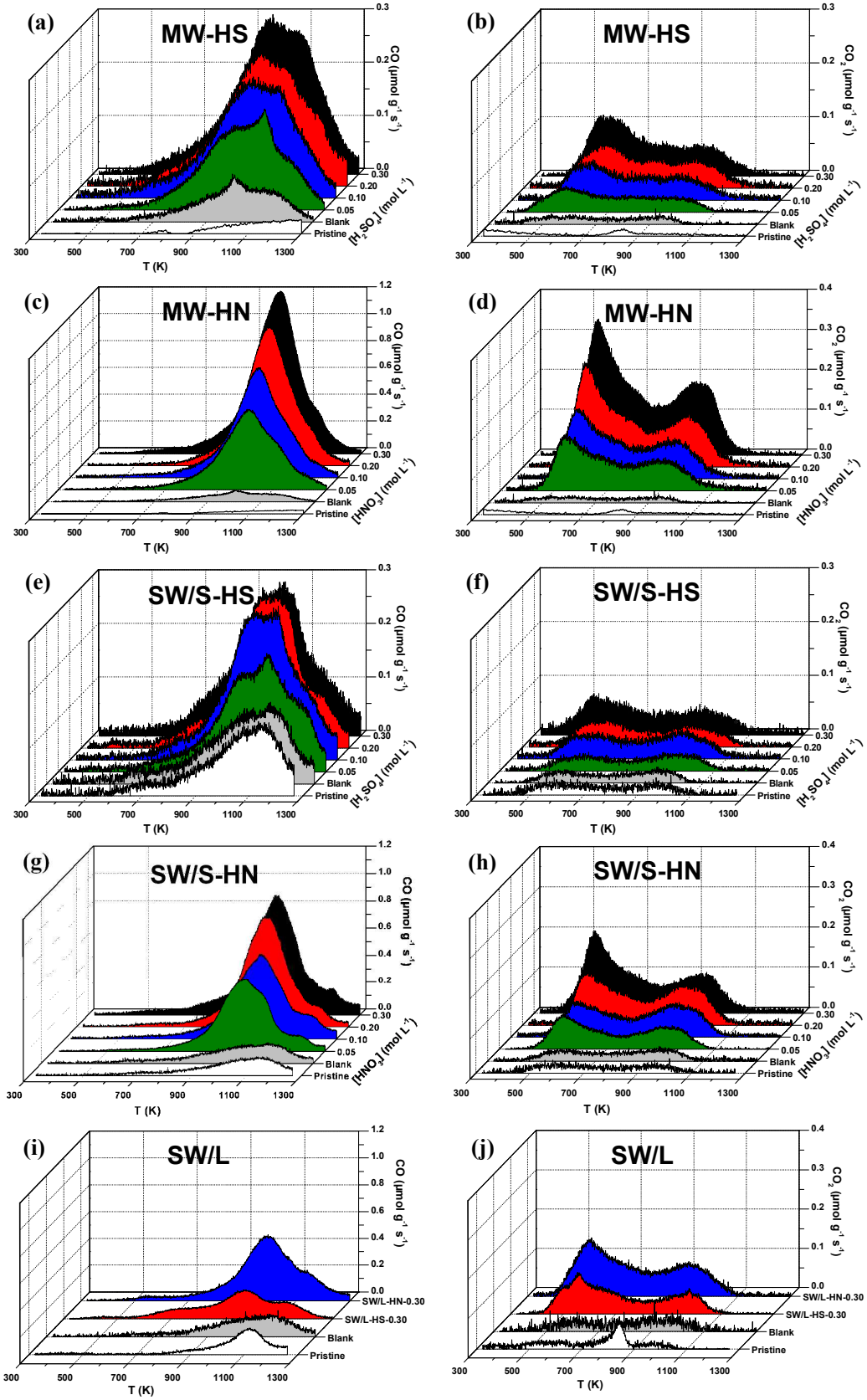

Figure 2. TPD spectra for pristine, blank (experiment with H_2O) and oxidized (a-d) MW, (e-h) SW/S and (i, j) SW/L, when using different (a, b, e, f) H_2SO_4 and (c, d, g, h) HNO_3 concentrations: (a, c, e, g, i) CO and (b, d, f, h, j) CO_2 desorption. TPD spectra for treated SW/L samples were obtained at 0.30 mol L^{-1} of acid concentration.

An experiment was also carried out with MW treated with the highest H_2SO_4 concentration but without adding $(NH_4)_2S_2O_8$ (labelled as MW-HS-0.30* in Table 3). Comparing with MW treated with H_2SO_4 plus $(NH_4)_2S_2O_8$ (MW-HS-0.30), the results showed a two-fold lower amount of CO (625 μmol g^{-1} for MW-HS-0.30* vs. 1312 μmol g^{-1} for MW-HS-0.30) and CO_2 (169 μmol g^{-1} for MW-HS-0.30* vs. 471 μmol g^{-1} for MW-HS-0.30). Therefore, $(NH_4)_2S_2O_8$ enhances the oxidation of the surface of MW. This has already been reported in literature but using activated carbons and carbon aerogels,[39-41] a larger oxidation in these carbon materials being reached in contrast with the MW oxidized in the present work, which is indicative of the resistance and difficulty to oxidize the graphitic walls of CNTs.

Figures 3a and 3b show the amounts of CO and CO_2, as well as the O_2 content, for MW samples, as a function of the H_2SO_4 and HNO_3 concentrations, respectively. Once again a mathematical function describes the obtained data. These correlations could be useful to tune the surface chemistry of such materials. Regarding the SW/S materials (results summarized in Figures 2e-h and Table 3), the conclusions are quite similar to those obtained for MW; i.e., the amounts of CO and CO_2 depend on the oxidizing agent used (and respective concentration), the oxidation being higher in the case of the experiments performed with HNO_3 (Figures 2g and 2h) instead of H_2SO_4 (Figures 2e and 2f). For instance, the amounts of CO (484, 1134 and 2529 μmol g^{-1} for pristine SW/S, SW/S-HS-0.30 and SW/S-HN-0.30, respectively) and CO_2 (109, 347 and 725 μmol g^{-1} for pristine SW/S, SW/S-HS-0.30 and SW/S-HN-0.30, respectively) evolved were seven times larger with HNO_3 treatments compared with those related with pristine SW/S, and larger than with H_2SO_4. In addition, a mathematical function can also be fitted to the amounts of CO and CO_2, as well as to the O_2 content in SW/S treated samples, regardless of the oxidizing agent used (Figures 3c and 3d).

Table 3. Total amounts of CO, CO_2 and SO_2 released by TPD, O_2 content and pH of the point of zero charge (pH_{PZC}) for pristine, blank CNTs and treated CNTs.

Sample	CO_2 (±20 μmol g^{-1})	CO (±20 μmol g^{-1})	O_2 (±0.1 wt.%)	CO/CO_2	SO_2 (±20 μmol g^{-1})	pH_{PZC} (±0.1)
Pristine MW	31	187	0.4	6.0	0	7.0
Blank MW	79	315	0.8	4.0	0	7.2
MW-HS-0.05	221	756	1.9	3.4	25	3.6
MW-HS-0.10	329	1040	2.7	3.2	45	3.1
MW-HS-0.20	421	1224	3.3	2.9	72	2.8
MW-HS-0.30	471	1312	3.6	2.8	81	2.6
MW-HS-0.30*	169	625	1.5	3.7	53	3.4
MW-HN-0.05	577	1900	4.9	3.3	0	6.1
MW-HN-0.10	694	2425	6.1	3.5	0	5.8
MW-HN-0.20	956	2901	7.7	3.0	0	5.2
MW-HN-0.30	1216	3335	9.2	2.7	0	4.4
Pristine SW/S	109	484	1.1	4.4	0	7.0
Blank SW/S	113	624	1.4	5.5	0	7.2
SW/S-HS-0.05	182	870	2.0	4.8	60	3.2
SW/S-HS-0.10	259	1104	2.6	4.3	92	2.6
SW/S-HS-0.20	284	1124	2.7	4.0	129	2.3
SW/S-HS-0.30	347	1134	2.9	3.3	144	2.2
SW/S-HN-0.05	341	1517	3.5	4.5	0	5.3
SW/S-HN-0.10	459	1908	4.5	4.2	0	4.8
SW/S-HN-0.20	604	2226	5.5	3.7	0	4.3
SW/S-HN-0.30	725	2529	6.4	3.5	0	4.1
Pristine SW/L	138	431	1.1	2.6	0	7.1
Blank SW/L	150	638	1.5	4.2	0	6.9
SW/L-HS-0.30	384	868	2.6	2.3	155	2.8
SW/L-HN-0.30	600	1603	4.5	2.7	0	4.7

MW-HS-0.30*: MW prepared with H_2SO_4 but without adding $(NH_4)_2S_2O_8$.

In the same line, the results obtained by TPD with the SW/L sample (treated with 0.30 mol L^{-1} of H_2SO_4 or HNO_3) are collected in Figures 2i and 2j and Table 3. Once again, the amounts of oxygenated functional groups are larger when the treatment is performed with HNO_3. For instance, the O_2 content (wt.%) increased in this order: pristine SW/L (1.1%) < SW/L-HS-0.30 (2.6%) < SW/L-HN-0.30 (4.5%).

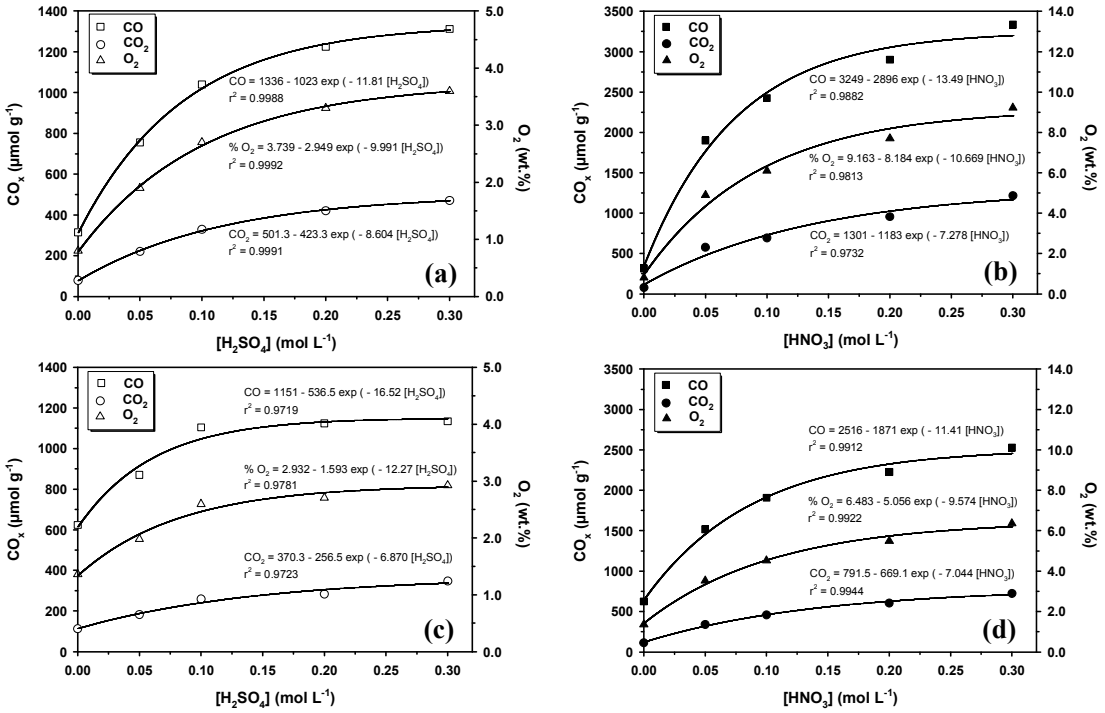

Figure 3. Evolution of the amounts of CO and CO_2, as well as O_2 content (determined by TPD) for (a, b) MW and (c, d) SW/S oxidized with different (a, c) H_2SO_4 and (b, d) HNO_3 concentrations.

The amounts of CO and CO_2 for the different CNTs were plotted (Figures 4a and 4b, respectively) as a function of the [acid]/m_{CNT} ratio (i.e., independent of the CNTs loading), where m_{CNT} represents the CNTs mass loaded in the autoclave (0.2 g). Overall, the amount of CO followed the order: MW > SW/S > SW/L regardless the HNO_3 concentration used. In contrast, the results found when the different CNTs were treated with H_2SO_4 were quite similar, with only a lower amount of CO being incorporated for SW/L (Figure 4a). Regarding the amount of CO_2 (Figure 4b), the order of CO_2 was similar to that of CO, namely: MW > SW/S > SW/L for HNO_3 treatments (regardless of the acid concentration used) and quite similar for H_2SO_4 treatments. An experiment performed with 0.4 g of CNTs (instead of 0.2 g) at 0.30 mol L^{-1} of HNO_3 confirms that the amounts of CO and CO_2 depend on the [acid]/m_{CNT} ratio.

Taking into account these results, it can be concluded that MW are more susceptible to the incorporation of oxygenated functional groups, independently of the kind of oxidizing agent used, and the amount of CO_2 is more affected than that of CO, suggesting the higher

production of more acidic surface groups, as commonly observed with acid driven treatments. The higher oxidation of MW, compared with both SW/S and SW/L, could be related with the fact that the structure of MWCNTs allows a larger number of defects where the oxidation process can be initiated[42] and, as consequence, yielding more functional groups during the oxidation treatment. The surface of SW/S was more easily modified than that of SW/L, mainly when HNO_3 is used as oxidant, the production of defects on SWCNTs (where the oxygenated functional groups are located) being expected to be difficult without simultaneously opening these CNTs.[42, 43] In general, it seems that thicker and shorter CNTs offer more reactive sites for surface functionalization, in agreement with our previous publication where two different MW samples were tested.[19]

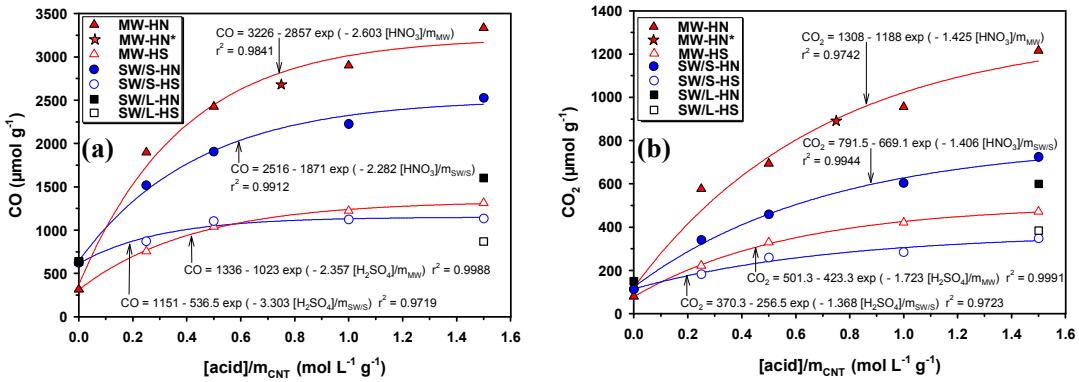

Figure 4. Evolution of the amounts of (a) CO and (b) CO_2 as a function of $[acid]/m_{CNT}$ for MW, SW/S and SW/L treated with H_2SO_4 and HNO_3 (m_{CNT} = 0.2 g). MW-HN* corresponds to a MW sample prepared with 0.30 mol L^{-1} of HNO_3 and 0.4 g of CNTs.

3.4. Analysis of sulphur-containing functional groups and measurement of the pH_{PZC}

The determination of the pH_{PZC} gives information on the different acidity of the samples. Thus, the evolution of the pH_{PZC} with the acid concentration was studied and presented in Figure 5 and Table 3, showing that an increase in acid concentration produces materials with more acidic character (e.g., pH_{PZC} is 7.0, 5.8 and 4.4, for pristine MW, MW-HN-0.10 and MW-HN-0.30, respectively). The functionalization of CNTs with H_2SO_4 leads to more acidic samples than those obtained with HNO_3 (i.e., pH_{PZC} is 2.6 and 5.2 for MW-HS-0.30 and MW-HN-0.30, respectively), although those treated with H_2SO_4 presented a lower amount of

oxygenated groups and a slightly higher CO/CO_2 ratio (2.8 and 2.7, for MW-HS-0.30 and MW-HN-0.30, respectively). The strong acidic character of materials treated with H_2SO_4 (and $(NH_4)_2S_2O_8$) has been reported in literature for activated carbon and explained by the incorporation of functional groups with higher acidity.[44]

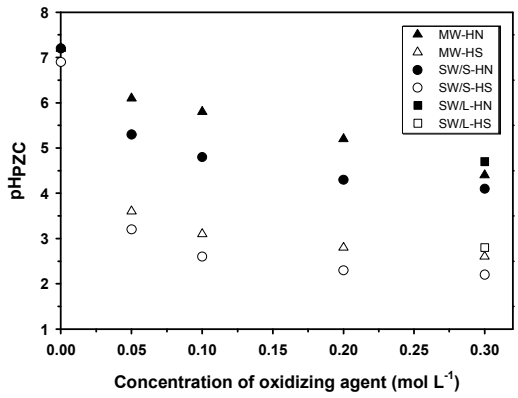

Figure 5. pH_{PZC} for MW and SW/S treated at different H_2SO_4 and HNO_3 concentrations. The pH_{PZC} obtained for SW/L treated with different acids (0.30 mol L^{-1}) are also included for comparison.

SW/S treated with HNO_3 were more acidic than MW and, then, SW/L, regardless of the acid concentration used (e.g., pH_{PZC} is 2.2, 2.6 and 2.8, for SW/S-HS-0.30, MW-HS-0.30 and SW/L-HS-0.30, respectively). The different acidic character can be explained by the incorporation of different kinds and amounts of acidic groups, which normally can be roughly evaluated with the CO/CO_2 ratio. For instance, MW treated with HNO_3 presented the lowest CO/CO_2 ratio but not the highest acidic character, probably because some acidic oxygenated groups (phenols) are evolved as CO (as verified below).

Since sulphur-containing functional groups, with a strong acid nature, have been reported for carbon materials treated with H_2SO_4,[32, 45, 46] the amounts of SO and SO_2 released during TPD were analysed, and the results are shown in Table 3 and Figure 6a. The incorporation of sulphur-containing functional groups was observed for all the CNTs treated with H_2SO_4, and larger amounts of SO_2 were obtained with increasing acid concentrations. Both pristine and blank CNTs did not present this type of functional groups (Table 3) and thus, these groups are created due to the oxidizing agent employed. Different amounts of SO_2 were

detected depending on the kind of the CNTs treated, SW/L and SW/S presenting higher amounts than those recorded for treated MW (e.g., 155, 144 and 81 μmol g^{-1} for SW/L-HS-0.30, SW/S-HS-0.30 and MW-HS-0.30, respectively). Figure 6b shows these results as a function of the [acid]/m_{CNT} ratio. A mathematical function can be also fitted to the amount of SO_2, which could be useful to tailor the surface chemistry of carbon materials and represents an advance not reported so far in the literature for this specific type of groups.

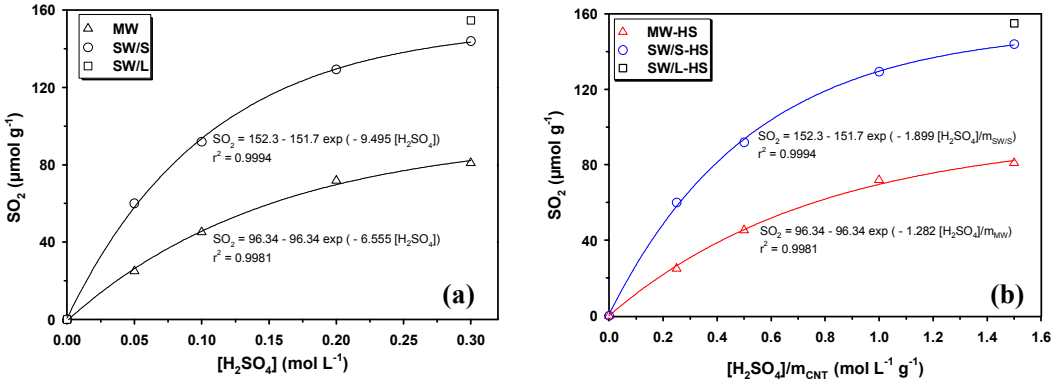

Figure 6. Evolution of the (a) amount of SO_2 determined by TPD, and (b) as a function of [H_2SO_4]/m_{CNT}, for MW and SW/S oxidized with different H_2SO_4 concentrations. The amount of SO_2 evolved for SW/L treated with H_2SO_4 (0.30 mol L^{-1}) is also included for comparison.

On the other hand, it is noteworthy that the amounts of sulphur-containing functional groups incorporated on the CNTs surface were lower than those of oxygen-containing groups. In addition, the use of $(NH_4)_2S_2O_8$ allows increasing the amount of SO_2 evolved (i.e., 81 and 51 μmol g^{-1} for MW-HS-0.30 and MW-HS-0.30*, respectively). Therefore, combination of H_2SO_4 and $(NH_4)_2S_2O_8$ enhanced the incorporation of oxygen- and sulphur-containing functional groups in comparison to H_2SO_4 alone.

The SO_2 peak recorded in TPD spectra (not shown) for all CNTs was released at temperatures between 485 and 615 K, and it seems to be attributed to some specific sulphur-containing groups, such as sulfonic acids.[46] The thermal decomposition of more stable sulphur-containing functional groups, such as sulphoxides and sulphones, occurs at higher temperatures (between 633 – 700 K).[46] Sulfonic acid groups are very strong acids (pK_a = – 6.5),[47] which

would justify the lower pH_{PZC} obtained for the CNTs treated with H_2SO_4 compared with the CNTs oxidized with HNO_3. In addition, this kind of groups observed for SW/S treated with H_2SO_4 could also corroborate the lower pH_{PZC} values observed for these samples, although a detailed and precise identification and quantification of the oxygenated groups could be useful to explain these differences in acidity.

3.5. Identification and quantification of the different oxygenated functional groups

In order to obtain more detailed information about the different oxygenated groups incorporated with the different acids and on the distinct CNTs, deconvolution of the TPD spectra was carried out for samples treated with 0.30 mol L^{-1} of both HNO_3 and H_2SO_4. The results are summarized in Tables S1 and S2 and in Figure 7. The deconvolution methodology was applied considering the temperatures at which the different groups are evolved as CO and CO_2 upon heating and some assumptions were made in accordance to the methodology previously reported elsewhere.[30, 31]

In general, carboxylic acid groups (evolved as CO_2, peaks #1 and #2) and phenolic groups (evolved as CO, peak #4) were the most relevant oxygenated groups created in the surface of both MW and SW samples, regardless of the acid used in the oxidation treatments (Tables S1 and S2, respectively for CO_2 and CO). On the other hand, the treatments performed with H_2SO_4 introduced a larger amount of anhydrides (evolved as CO and CO_2, peak #3) than the oxidation performed with HNO_3. For SW/S and SW/L, a larger amount of strong carboxylic acid groups (evolved as CO_2, peak #1) was detected in comparison to MW samples, regardless of the acid used which could also justify the lower pH_{PZC} (Table 3) obtained for SW/S treated with HNO_3. On the other hand, the amount of anhydrides, lactones (evolved as CO_2, peak #4) and mainly carbonyl/quinones (evolved as CO, peaks #5 and #6) where larger in the case of treated SW/L in comparison with treated SW/S, for both oxidizing agents. On the contrary, the incorporation of phenol groups was larger in the case of SW/S, regardless of the acid used in these treatments.

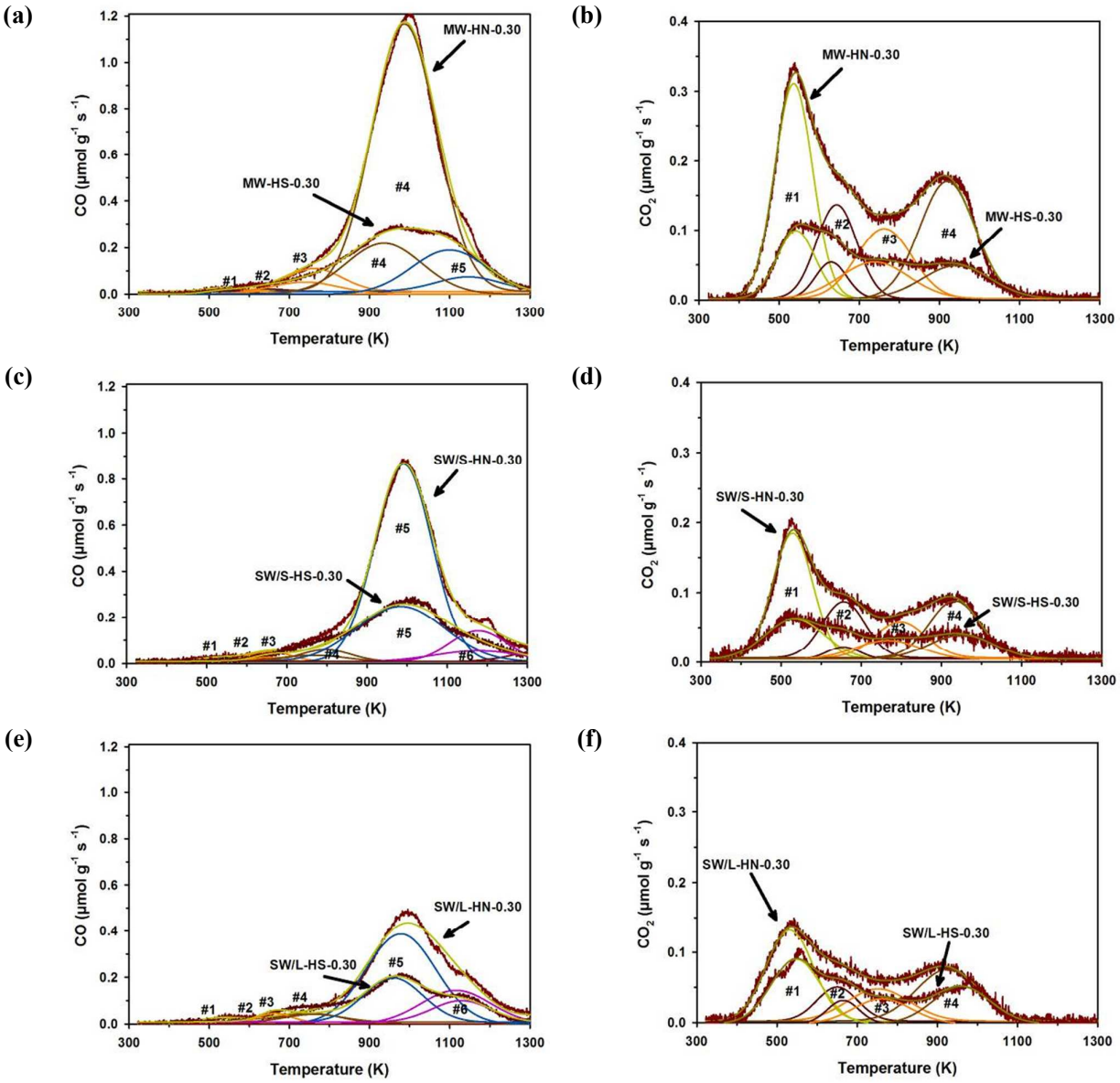

Figure 7. Deconvolution of TPD spectra for (a, b) MW, (c, d) SW/S and (e, f) SW/L treated with HNO_3 and H_2SO_4 (0.30 mol L^{-1}): (a, c, e) CO and (b, d, f) CO_2.

3.6. Direct contact membrane distillation by using PTFE membranes modified with CNTs

Pristine MW, SW/S and SW/L and the corresponding samples oxidized with the highest HNO_3 concentration tested (0.30 mol L^{-1}) were used to prepare the BP membranes. Figures 8a and 8b respectively show photographs of a bare PTFE commercial membrane and a BP membrane (the later prepared with the MW-HN-0.30 sample). In fact, a homogeneous layer of CNTs (free of defects and cracks) was always obtained onto the PTFE membrane. The BP membranes prepared were firstly tested in DCMD by using DI water as feed and the results are

shown in Figure 8c. The permeate fluxes obtained with BP membranes prepared with pristine MW, SW/S and SW/L (i.e., 7.3, 9.6 and 6.5 kg m^{-2} s^{-1}, respectively) were always lower than that determined with the PTFE membrane (10.4 kg m^{-2} s^{-1}). The parameters usually affecting the distillation performance are related with the morphology (pore size, porosity, thickness, tortuosity and roughness), surface energy (hydrophobicity) and thermal conductivity of the membrane.[24] Dumée et al.[48] have recently shown that, for BP membranes with similar geometric properties (porosity or pore size distribution), the permeation of water vapour as well as salt rejection were enhanced for membranes with lower surface energy (i.e., higher hydrophobicity, as determined by higher contact angles). The authors suggested that higher hydrophobicity leads to increased vapour transport due to reduced heat transfer. This effect is not predicted by conventional membrane distillation theory (Knüdsen diffusion), which is only focused on geometric measurable parameters of the membranes. Therefore, in the present work, the lower pore size and hydrophobicity of the BP membranes in comparison with the PTFE membrane can justify the lower permeate fluxes obtained with BPs.

Among the BP membranes tested, that prepared with pristine SW/S presented a higher permeate flux than those prepared with pristine MW and with pristine SW/L. Taking into account that all these pristine CNTs presented negligible amounts of functional groups, the different behaviours found should be related with the length, diameter and packing of the CNTs, as well as with the type of interaction between CNTs and the PTFE support, including possible incorporation of CNTs into the pores of the PTFE support, providing different pathways for the transport of water vapour molecules.[49]

A significant increase of the permeate flux was observed when using the BP membrane prepared with oxidized MW (i.e., 11.6 kg m^{-2} s^{-1} for the BP membrane prepared with MW-HN-0.30). This increase in the flux was already observed for BPs supported on polypropylene membranes and explained by the positive influence of the polar groups on vapour permeability, while preventing liquid penetration into the membrane pores.[20] Therefore, hydrothermal oxidation seems to create polar surface groups which provide higher sorption of the water

vapour molecules. The increase of permeate flux was also notorious for the BP membrane prepared with SW/L-HN-0.30 (8.3 kg m^{-2} s^{-1}), but negligible in the case of BP membranes prepared with pristine and oxidized SW/S, these CNTs leading to a high permeate flux even when they are not oxidized.

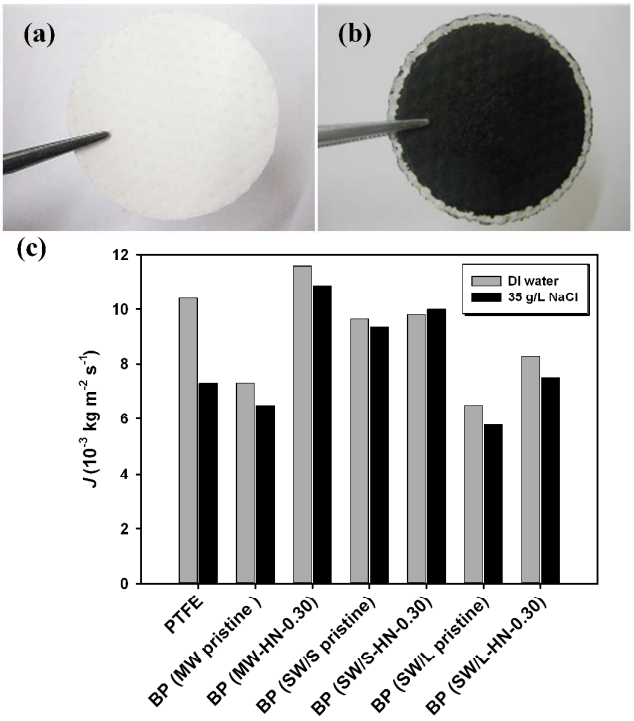

Figure 8. Photographs of (a) PTFE and (b) BP membrane prepared with the MW-HN-0.30 sample. (c) Permeate flux (*J*) obtained when using DI (light bars) or salty (dark bars) water as feed for different membranes (PTFE and BPs with pristine and oxidized CNTs).

When a NaCl solution with a concentration similar to that of seawater was used as feed in DCMD, the permeate flux generally decreased, the largest difference being observed with the commercial membrane (from 10.6 to 7.3 kg m^{-2} s^{-1}, with DI and salty water, respectively). However, under these salinity conditions, all the BP membranes prepared with oxidized CNTs presented a higher permeate flux than the commercial membrane (with little influence in the case of SW/S). In the case of BP membranes prepared with pristine CNTs, the permeate flux was 9.4 > 6.5 > 5.8 kg m^{-2} s^{-1} for SW/S > MW > SW/L, respectively, while for BP membranes prepared with oxidized CNTs, the flux was 10.9 > 10.0 > 7.5 kg m^{-2} s^{-1} for MW > SW/S > SW/L, respectively. Therefore, under salinity conditions, the oxidized CNTs, but in particular

the oxidized MW, significantly increased the efficiency of the commercial membrane without affecting the salt rejection (always found as 100.0 %).

In order to study the effect of the controlled functionalization of the CNTs surface on permeate flux, BP membranes prepared with MW oxidized with different HNO_3 concentrations were tested in DCMD by using salty water as feed (Figure 9a). The permeate flux determined for the BP membranes corroborated the beneficial effect of the oxygenated surface groups on the behaviour of these membranes in DCMD. In fact, this flux seems to be related with the oxygenated surface groups created in the CNTs by controlled oxidation.

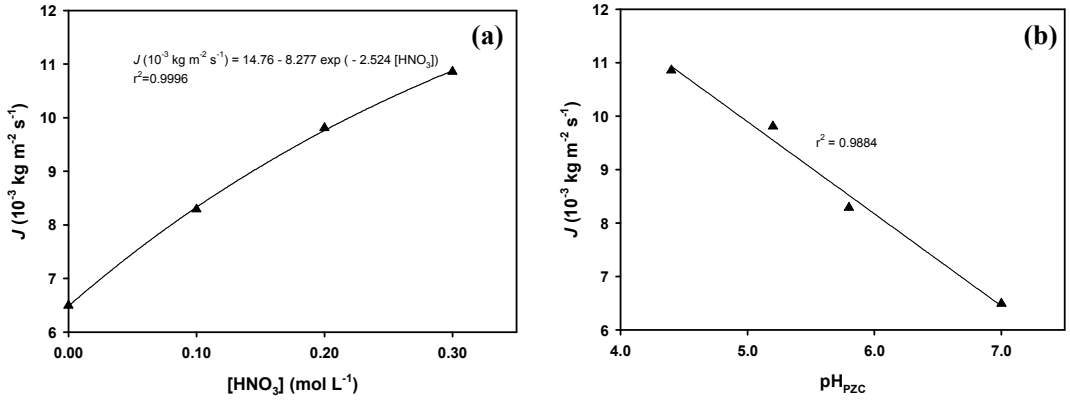

Figure 9. Influence of (a) HNO_3 concentration and (b) pH_{PZC} of MW samples on the permeate flux (J) of BP membranes.

In addition, a linear correlation was found with respect to the pH_{PZC} (Figure 9b); an increase of the permeate flux is systematically obtained with an increase of the acidic character of CNTs. This improvement of the permeate flux, while observing complete salt rejection, could be due to pronounced repulsive electrostatic interactions established between chloride ions and the negatively charged surface of the acidic membranes, which will favour the flux in salty conditions, in agreement with studies performed with other carbon-based membranes.[50, 51]

4. Conclusions

The surface chemistry of CNTs can be controlled by the hydrothermal oxidation methodology, by using different oxidizing agents and varying their respective concentrations.

Regarding the textural properties, the oxidations performed with HNO_3 have a more relevant effect than those carried out with H_2SO_4, a decrease of the total pore volume and average pore diameter of CNT bundles being, in general, observed. Concerning the surface chemical properties, the amounts of CO, CO_2 and SO_2 as well as the O_2 content (determined by TPD analysis and directly related with the amount of surface functional groups) can be correlated to the oxidizing agent concentration by using mathematical functions.

The amount of oxygen-containing surface groups depends on the morphology of CNTs (number and length of graphene layers), more surface groups being found for MWCNTs, followed by short SWCNTs and then by long SWCNTs, regardless of the oxidizing agent at any fixed concentration. Therefore, thicker and shorter CNTs seem to offer more reactive sites for surface functionalization with oxygen-containing groups than thinner and longer CNTs. For a specific type of CNTs, the amount of surface oxygenated groups released as CO and CO_2 is always larger with HNO_3 than with H_2SO_4. In general, carboxylic acid and phenol groups were the major oxygenated surface groups created in CNTs.

Sulphur-containing groups were also detected when using H_2SO_4, larger amounts of these groups being found in SWCNTs than in MWCNTs. Short SWCNTs are more acidic than MWCNTs, regardless of the oxidizing agent at any fixed concentration. In addition, all the CNTs oxidized with H_2SO_4 presented more acidic character than those obtained with HNO_3 due to the strong acidic character of the sulphur-containing groups. Overall, both HNO_3 and H_2SO_4 hydrothermal oxidation methodologies were found to be efficient for the precise control of the amount and type of surface groups in CNTs.

Buckypapers prepared with MWCNTs oxidized with HNO_3 significantly improved the permeate flux of PTFE membranes under salinity conditions, preserving complete salt rejection. Mathematical correlations between the flux and oxygenated surface groups (as well as pH_{PZC}) where found. The highest flux was obtained when using BP membranes prepared with the most acidic MWCNTs, i.e. those with the highest amount of surface groups. This improvement on the flux could be due to the electrostatic repulsions between chloride ions and

the negatively charged surface of the MWCNTs and to a better affinity of water vapour to the membrane. The results of this study demonstrate how the presence and amount of functional groups in CNTs can improve the performance of hydrophobic commercial membranes commonly applied to water desalination by DCMD.

Acknowledgments

Financial support for this work was provided by project PTDC/AAC-AMB/122312/2010 co-financed by FCT (Fundação para a Ciência e a Tecnologia) and FEDER through Programe COMPETE (FCOMP-01-0124-FEDER-019503). This work was also supported by FCT and FEDER through project PEst-C/EQB/LA0020/2013 under Programe COMPETE, and by QREN, ON2 and FEDER through project NORTE-07-0162-FEDER-000050. AMTS acknowledges the FCT Investigator 2013 Programme (IF/01501/2013), with financing from the European Social Fund and the Human Potential Operational Programme. SMT and LMPM acknowledge financial support from SFRH/BPD/74239/2010 and SFRH/BPD/88964/2012, respectively.

References

1. S. Iijima, *Nature*, 1991, **354**, 56-58.
2. P. Serp and J. L. Figueiredo, *Carbon materials for catalysis*, John Wiley & Sons, New Jersey, 2009.
3. M. M. Pendergast and E. M. V. Hoek, *Energy & Environmental Science*, 2011, **4**, 1946-1971.
4. B. Corry, *Energy & Environmental Science*, 2011, **4**, 751-759.
5. S. C. Tsang, P. J. F. Harris and M. L. H. Green, *Nature*, 1993, **362**, 520-522.
6. D. B. Mawhinney, V. Naumenko, A. Kuznetsova, J. T. Yates, J. Liu and R. E. Smalley, *Journal of the American Chemical Society*, 2000, **122**, 2383-2384.
7. I. D. Rosca, F. Watari, M. Uo and T. Akasaka, *Carbon*, 2005, **43**, 3124-3131.

8. M. T. Martínez, M. A. Callejas, A. M. Benito, M. Cochet, T. Seeger, A. Ansón, J. Schreiber, C. Gordon, C. Marhic, O. Chauvet, J. L. G. Fierro and W. K. Maser, *Carbon*, 2003, **41**, 2247-2256.

9. C. G. Salzmann, S. A. Llewellyn, G. Tobias, M. A. H. Ward, Y. Huh and M. L. H. Green, *Advanced Materials*, 2007, **19**, 883-887.

10. F. Avilés, J. V. Cauich-Rodríguez, L. Moo-Tah, A. May-Pat and R. Vargas-Coronado, *Carbon*, 2009, **47**, 2970-2975.

11. S. Hanelt, G. Orts-Gil, J. F. Friedrich and A. Meyer-Plath, *Carbon*, 2011, **49**, 2978-2988.

12. K. J. Ziegler, Z. Gu, H. Peng, E. L. Flor, R. H. Hauge and R. E. Smalley, *Journal of the American Chemical Society*, 2005, **127**, 1541-1547.

13. V. Datsyuk, M. Kalyva, K. Papagelis, J. Parthenios, D. Tasis, A. Siokou, I. Kallitsis and C. Galiotis, *Carbon*, 2008, **46**, 833-840.

14. J. Chen, Q. Chen and Q. Ma, *Journal of Colloid and Interface Science*, 2012, **370**, 32-38.

15. S. W. Kim, T. Kim, Y. S. Kim, H. S. Choi, H. J. Lim, S. J. Yang and C. R. Park, *Carbon*, 2012, **50**, 3-33.

16. A. M. T. Silva, B. F. Machado, J. L. Figueiredo and J. L. Faria, *Carbon*, 2009, **47**, 1670-1679.

17. R. R. N. Marques, B. F. Machado, J. L. Faria and A. M. T. Silva, *Carbon*, 2010, **48**, 1515-1523.

18. G. E. Romanos, V. Likodimos, R. R. N. Marques, T. A. Steriotis, S. K. Papageorgiou, J. L. Faria, J. L. Figueiredo, A. M. T. Silva and P. Falaras, *The Journal of Physical Chemistry C*, 2011, **115**, 8534-8546.

19. V. Likodimos, T. A. Steriotis, S. K. Papageorgiou, G. E. Romanos, R. R. N. Marques, R. P. Rocha, J. L. Faria, M. F. R. Pereira, J. L. Figueiredo, A. M. T. Silva and P. Falaras, *Carbon*, 2014, **69**, 311-326.

20. M. Bhadra, S. Roy and S. Mitra, *Separation and Purification Technology*, 2013, **120**, 373-377.

21. L. F. Dumée, K. Sears, J. Schütz, N. Finn, C. Huynh, S. Hawkins, M. Duke and S. Gray, *Journal of Membrane Science*, 2010, **351**, 36-43.

22. L. Dumée, J. L. Campbell, K. Sears, J. Schütz, N. Finn, M. Duke and S. Gray, *Desalination*, 2011, **283**, 64-67.

23. L. Dumée, K. Sears, J. Schütz, N. Finn, M. Duke and S. Gray, *Desalination and Water Treatment*, 2010, **17**, 72-79.

24. L. Camacho, L. Dumée, J. Zhang, J.-d. Li, M. Duke, J. Gomez and S. Gray, *Water*, 2013, **5**, 94-196.

25. S. Brunauer, P. H. Emmett and E. Teller, *Journal of the American Chemical Society*, 1938, **60**, 309-319.

26. E. P. Barrett, L. G. Joyner and Halenda, *Journal of the American Chemical Society*, 1951, **73**, 373-380.

27. A. V. Neimark, Y. Lin, P. I. Ravikovitch and M. Thommes, *Carbon*, 2009, **47**, 1617-1628.

28. J. Rivera-Utrilla, I. Bautista-Toledo, M. A. Ferro-García and C. Moreno-Castilla, *Journal of Chemical Technology & Biotechnology*, 2001, **76**, 1209-1215.

29. L. M. Pastrana-Martínez, S. Morales-Torres, S. K. Papageorgiou, F. K. Katsaros, G. E. Romanos, J. L. Figueiredo, J. L. Faria, P. Falaras and A. M. T. Silva, *Applied Catalysis B: Environmental*, 2013, **142-143**, 101-111.

30. J. L. Figueiredo, M. F. R. Pereira, M. M. A. Freitas and J. J. M. Órfão, *Carbon*, 1999, **37**, 1379 - 1389.

31. J. L. Figueiredo, M. F. R. Pereira, M. M. A. Freitas and J. J. M. Órfão, *Industrial & Engineering Chemistry Research*, 2007, **46**, 4110-4115.

32. H. T. Gomes, S. M. Miranda, M. J. Sampaio, A. M. T. Silva and J. L. Faria, *Catalysis Today*, 2010, **151**, 153-158.

33. R. M. Smith and K. L. Busch, *Understanding Mass Spectra - A Basic Approach*, John Wiley & Sons, 1999.

34. H. Yu, Y. Jin, F. Peng, H. Wang and J. Yang, *The Journal of Physical Chemistry C*, 2008, **112**, 6758-6763.

35. R. C. Bansal, J. B. Donnet and F. Stoeckli, *Active Carbon*, Marcel Dekker, New York, 1988.

36. M.-K. Seo and S.-J. Park, *Current Applied Physics*, 2010, **10**, 241-244.

37. W.-F. Du, L. Wilson, J. Ripmeester, R. Dutrisac, B. Simard and S. Dénommée, *Nano Letters*, 2002, **2**, 343-346.

38. I. A. A. C. Esteves, F. J. A. L. Cruz, E. A. Müller, S. Agnihotri and J. P. B. Mota, *Carbon*, 2009, **47**, 948-956.

39. N. Li, X. Ma, Q. Zha, K. Kim, Y. Chen and C. Song, *Carbon*, 2011, **49**, 5002-5013.

40. S. Morales-Torres, F. J. Maldonado-Hódar, A. F. Pérez-Cadenas and F. Carrasco-Marín, *Journal of Hazardous Materials*, 2010, **183**, 814-822.

41. C. Moreno-Castilla, M. A. Ferro-Garcia, J. P. Joly, I. Bautista-Toledo, F. Carrasco-Marin and J. Rivera-Utrilla, *Langmuir*, 1995, **11**, 4386-4392.

42. Y.-C. Chiang, W.-H. Lin and Y.-C. Chang, *Applied Surface Science*, 2011, **257**, 2401-2410.

43. J. Zhang, H. Zou, Q. Qing, Y. Yang, Q. Li, Z. Liu, X. Guo and Z. Du, *The Journal of Physical Chemistry B*, 2003, **107**, 3712-3718.

44. C. Moreno-Castilla, M. V. López-Ramón and F. Carrasco-Marin, *Carbon*, 2000, **38**, 1995 - 2001.

45. Y. Wang, Z. Iqbal and S. Mitra, *Journal of the American Chemical Society*, 2005, **128**, 95-99.

46. A. P. Terzyk, *Journal of Colloid and Interface Science*, 2003, **268**, 301-329.

47. T. W. G. Solomons and C. B. Fryhle, *Organic Chemistry*, John Wiley & Sons, New Jersey, 2011.

48. L. F. Dumée, S. Gray, M. Duke, K. Sears, J. Schütz and N. Finn, *Desalination*, 2013, **323**, 22-30.

49. K. Gethard, O. Sae-Khow and S. Mitra, *ACS Applied Materials & Interfaces*, 2010, **3**, 110-114.

50. D. Konatham, J. Yu, T. A. Ho and A. Striolo, *Langmuir*, 2013, **29**, 11884-11897.

51. W.-F. Chan, H.-y. Chen, A. Surapathi, M. G. Taylor, X. Shao, E. Marand and J. K. Johnson, *ACS Nano*, 2013, **7**, 5308-5319.